Rev.Adv.Mater.Sci. 25 (2010) 194-202

FEATURES OF DEFORMATION BEHAVIOR AT ROLLING AND TENSION UNDER CURRENT IN TiNi ALLOY

V.V. Stolyarov[1,2]

[1]Mechanical Engineering Research Institute of Russian Academy of Science,
Maly Kharitonievsky lane, 4, 101990, Moscow, Russia
[2]Moscow State Industrial University, Avtozavodskaya St., 16, 115280, Moscow, Russia

Received: November 21, 2009

Abstract. The paper presents data on the effect of pulse current on deformability, strength and ductility of a shape-memory TiNi alloy processed by electroplastic rolling (EPR). It has been found that deformability and elongation to failure can be enhanced by electropulse current. The deformation behavior of the TiNi alloy both at EPR processing and tension with pulse current is considered. It is shown that EPR significantly increases strain to failure and refines microstructure to a grain size under 100 nm. Stress jumps upward and downward have been observed on the stress-strain curves at tension with current. Different directions of stress jumps are conditioned by the martensite transformation and the electroplastic effect, correspondingly.

1. INTRODUCTION

Recently for enhancing ductility in submicrocrystalline (SMC) and nanocrystalline (NC) materials methods based on structure design have been offered [1-3]. Another approach that can also be considered as a method for increasing technological ductility is electropulse treatment (EPT), as well as electroplastic deformation (EPD) [4,5]. For example, an essential increase in elongation without a decline in strength after EPT of brittle magnesium AZ61 alloy is demonstrated in [5], and a method of application of the electroplastic effect is shown in [4].

A special place among new materials belongs to shape-memory TiNi-based alloys. In coarse-crystalline (CC) and microcrystalline (MC) states they possess sufficiently high ductility (40-60%). This can be explained by thermoelastic martensitic transformation caused by temperature, stress or strain change [6]. Nanostructuring of such alloys provides enhancement of strength properties, as well as functional ones – recovery stress and maximum completely recoverable strain [7]. Earlier it was shown that EPD is one of severe plastic deformation techniques allowing to produce nanostructure in TiNi alloys [8]. Therefore, it would be important to know how deformability and ductility change in an EPD-processed TiNi alloy. The present paper is devoted to investigation of the effect of pulse current on deformability and ductility of a shape-memory TiNi alloy processed by EPD.

Corresponding author: V.V. Stolyarov, e-mail: vlstol@mail.ru

2. EXPERIMENTAL PROCEDURE AND MATERIALS

The initial $Ti_{49.4}Ni_{50.6}$ and $Ti_{49.3}Ni_{50.7}$ alloys with very similar compositions were subjected to quenching at 800 °C in cold water to obtain a CC structure with a mean grain size of 50 μm. Then the following techniques and technological combinations were employed to produce SMC and NC states: 1 – equal-channel angular pressing at 450 °C with eight passes (ECAP 450 °C (8)); 2 – high-pressure torsion at 5 revolutions (HPT (5)); 3 – multiple electroplastic rolling (EPR) of the CC alloy; and 4 - EPR of the SMC alloy on strips with the cross section 2x6 mm^2 under pulse unipolar current with current density j = 84-222 A/mm^2, pulse duration (8-10)x10^{-3} $s^{-1}$and frequency 10^3 Hz; the details of the method are described in [8]. After each pass the sample was cooled in water to avoid a significant heat effect. The deformability of the EPR-processed samples was estimated by true strain $e = \ln t_i / t_f$ (t_i, t_f - initial and final strip thickness) within the range of e = 0.5 - 2.0. The microstructure was investigated by TEM on specimens with annealing temperatures (T_{an}) of 450 and 550 °C that correspond to the structures of recrystallization and aging. Mechanical properties were studied during tension at room temperature and strain rate 0.5 mm/min (0.4x10^{-3} s^{-1}) on a MTS device (without current) and a horizontal IM-5081 machine (with single and multiple pulses current). During tension current densities were varied from 1500 to 3000 A/mm^2 and pulse duration was varied from 100 to 1000 ms. Temperature on the sample surface during injection of pulse current was measured by an infrared camera CEDIP Silver 450M with the accuracy 0.25° and the scanning frequency about 2 x 10^4 Hz within the range of 20 up to 500 °C. To clarify the capability of current for structure relaxation, EPT processing during 5 s at j =110 A/mm^2 was instead of furnace annealing for one experiment.

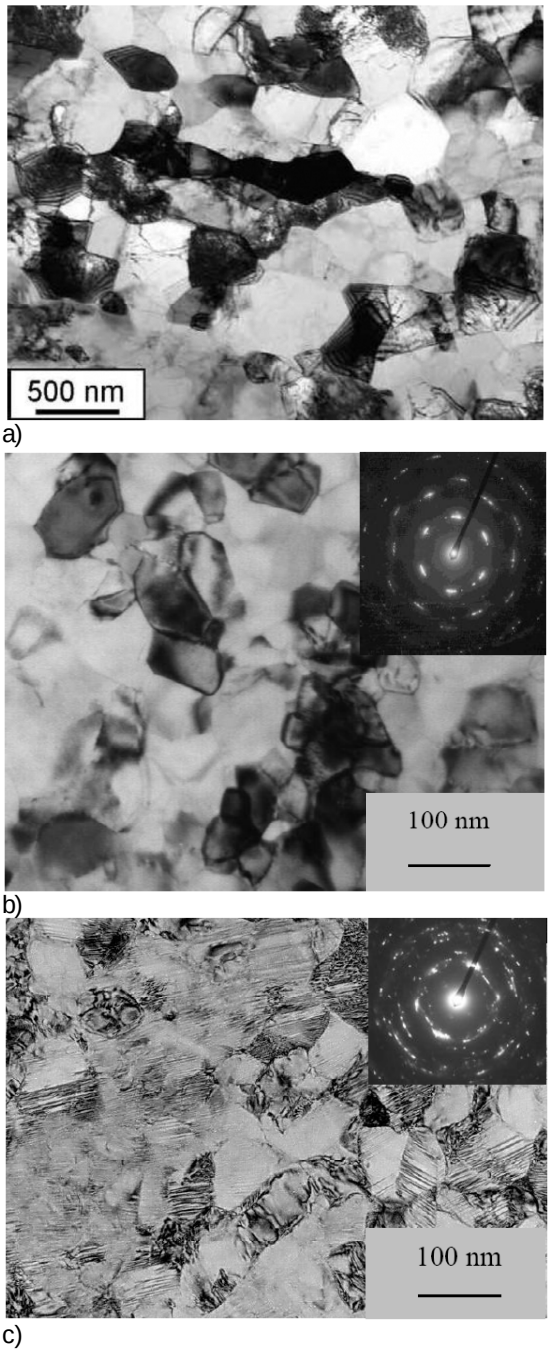

Fig. 1. Bright fields TEM micrographs of $Ti_{49.4}Ni_{50.6}$ alloy processed by ECAP (a), EPR (b) and ECAP + EPR (c) and the following annealing at 550 °C (a) and 450 °C (b,c) for 1 hour.

3. EXPERIMENTAL DATA

3.1. Microstructure

The results of TEM investigation of SPD-produced alloys processed by ECAP, EPR (e=1.81, j =168 A/mm^2), ECAP + EPR (e=1.91, j = 200 A/mm^2) and a subsequent post-deformation annealing have revealed formation of SMC or NC structures of the austenite B2 phase with a mean grain size of 600, 100, and 50 nm, correspondingly (Fig. 1). A detailed analysis of diffraction patterns for samples processed by EPR and ECAP + EPR before annealing shows that there are amorphous and $B19^2$ phases in a small fraction, and a crystallographic texture (200).

Another structural feature of these patterns consists in different intragranular defect structures. There is a high dislocation density within the grains and

Table 1. Deformability of alloys at cold rolling without and with a current.

Treatment	*Initial state*	*Current density, j* [A/mm^2]	*Strain to fracture, e*	*Fracture observation*
Quenching	CC	0	0.54	By separation
		60	0.55	By separation
		84	0.84	By single microcracks
		168	1.81	no
ECAP	SMC	0	0.59	by separation
		100	0.59	by single microcracks
		160	1.20	no
		200	1.91	no

at the grain boundaries of the ECAP-processed sample (Fig. 1a), whereas in the EPR-processed sample the grains have practically no lattice defects (Fig. 1b). On the contrary, the grains of the sample processed by ECAP + EPR have many thin microtwins of the B19'-phase (Fig. 1c). Thus the states after processing differ not only in grain size but also in phase composition and defect density. Note should be made that the EPR technique has transformed CC and SMC structures to NC structures with a close grain size.

3.2. Deformability

Deformability of the alloy at cold rolling with current is considerably higher than without current (Table 1). Deformability increases with increasing pulse current density for CC and SMC alloys. The maximum strain to fracture for CC and SMC alloys after cold rolling with current (e = 1.81-1.91) was three times higher than for the same alloys after cold rolling without current (e = 0.54 - 0.59). The effect of EPR depends on the structural state and begins at current density over 60 and 100 A/mm^2 for CC and SMC states, correspondingly.

The fracture type at cold rolling depends also on the mode of current. For the lack of current the fracture type is brittle with sample separation into parts (Fig. 2a). At current density over 60 A/mm^2 brittle fracture has not been observed. In this case cold rolling is accompanied by edge microcracks (Fig. 2b) which disappear with an increase in current density exceeding 100 A/mm^2.

3.3. Mechanical behavior and properties

3.3.1. Tension without current

The mechanical behavior of shape-memory TiNi alloys differs from that of traditional materials. The view of stress-strain curves depends on the relation of straining temperature T_s (T_s = RT in our case) and the temperatures of the start and the finish of transformation at cooling (M_s, M_f) or heating (A_s, A_f). For the $Ti_{49.3}Ni_{50.7}$ alloy in the quenched and EPR-processed states this relation corresponds to $M_s < T_s < A_f$. A typical tensile stress-strain curve at room temperature is shown in Fig. 3a. It can be seen that there is a yield stress plateau corresponding to reverse phase transformation A↔M. Beyond the plateau irreversible elastic-plastic martensite deformation is observed. Application of EPR processing leads to strong hardening and disappearance of a transformation plateau (Fig. 3b). A subsequent annealing at 450 °C resulted in recovery of the stress plateau at higher stress and to occurrence of an additional plateau at small stress (Fig. 3c).

The mechanical properties of the alloy subjected to EPR and a following annealing are presented in Table 2. For comparison, data for the quenched state, the states after ECAP [9,10] and HPT processing followed by annealing are given as well. These data demonstrate that the TiNi alloy in the NC state processed by EPR and a subsequent annealing has higher US, YS that in the CC and the SMC states. It can be seen that strength grows, but elongation to failure decreases with grain refinement, which is typical of the most materials. The highest strength and the smallest elongation to failure correspond to the NC state with a very small grain size. Ductility has been significantly improved

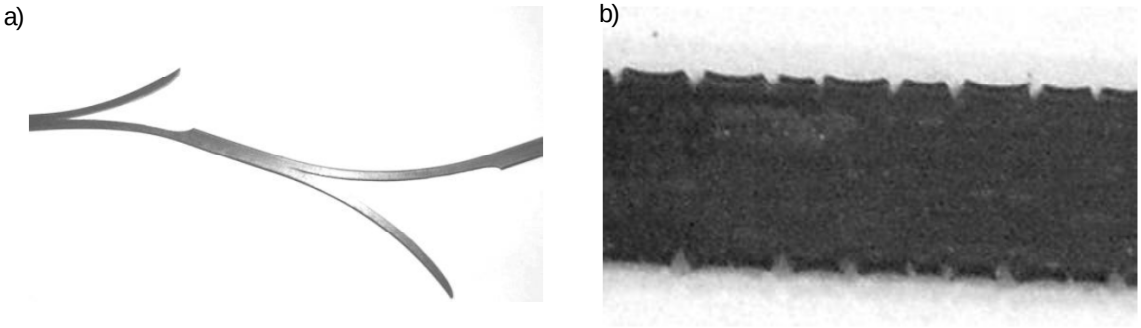

Fig. 2. Sample view after cold rolling without (a) and with (b) current.

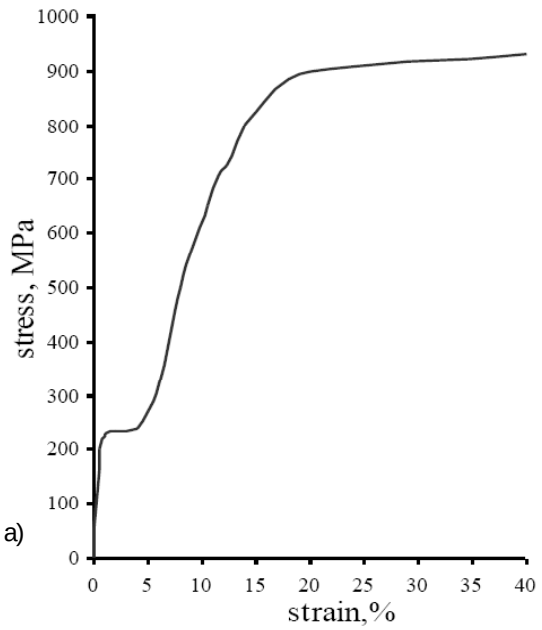

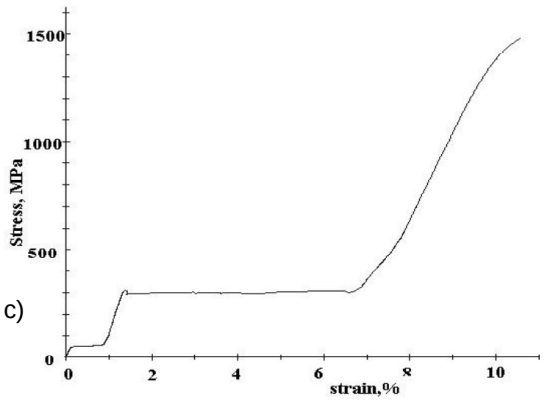

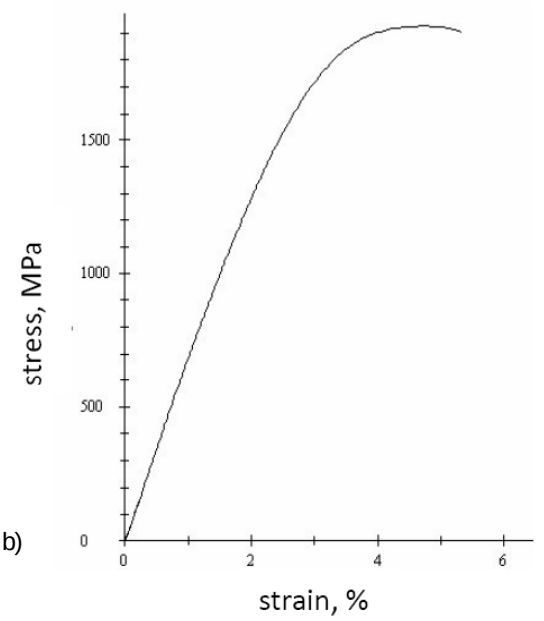

Fig. 3. Stress-strain curves for $Ti_{49,3}Ni_{50,7}$ alloy in CC (a) and и NC (b, c) states before (b) and after (c) annealing.

by post-deformation annealing at 200, 450, and 550 °C. Note that ε_m for the NC (8.1%) state is two times higher that for the CC (4.0%) and the SMC states (3.5%).

In Table 2 the mechanical properties of the EPR-processed alloy subjected to electropulse treatment (EPT) for 5 s at j =110 A/mm^2 instead of post-deformation annealing at 450 °C for 1 hour are given. A comparison of the mechanical properties of the EPR-processed alloy after both processing methods shows advantage of EPT both in strength and ductility.

Table 2. Mechanical properties at tension of the $Ti_{49.3}Ni_{50.7}$ alloy.

Treatment	*State*	*grain size*, [mm]	ε_m[%]	$\sigma_м$, [MPa]	YS [MPa]	UTS, [MPa]	δ, [%]
Quenching from 800 °C	CC	50	4	210	600	940	40
ECAP 450°C (8) + 550 °C	SMC	0.6	4.5	230	860	1150	25
ECAP 450 °C (8)	SMC	0.3	3.5	290	1140	1240	15
EPR (*e* = 1.81)	NC+A	0.08	–	–	1587	1926	2.4
EPR (*e* = 1.81) + 450 °C	NC	0.10	8.1	250	1200	1300	9.6
EPR (*e* =1.81)+EPT (5s, *j*=110 A/mm^2)	NC	0.10		500	1350	1550	10.5
ECAP + EPR (*e* = 1.91) + 450 °C	NC	0.05	5	294	1395	1481	8.0
HPT (5) + 200 °C	NC	0.02	–	320	1570	2650	<1

ε_m and ε_m – martensitic-induced transformation strain and stress

3.2.2. Tension with pulse current

The mechanical behavior at tension under single pulses current for the alloy after quenching, EPR (*e*=1.91, *j* = 200 A/mm^2, τ = 160 μs,) and EPR + 450 °C is shown in Fig. 4. The distinctive feature of stress-strain curves under pulse current is occurrence of stress jumps, each of which corresponds to a single current pulse. The jump direction (upward or downward) and the jump amplitude (25-300 MPa) depend both on structural state of the alloy and the mode of pulse current.

Stress jumps to a downward amplitude of less than 50 MPa have been observed only in the quenched CC alloy. They are placed beyond the stress plateau s_m after a yield stress point for martensite. The amplitude of stress jump increases slightly with increasing strain (Fig. 4a).

Stress jumps upward have been observed at $\sigma \geq \sigma_m$ for the CC and the NC states. The maximum stress jump amplitude of 200 MPa corresponds to the quenched alloy (Fig. 4a). The stress jump amplitude decreases from maximum to zero with increasing strain at *j* = 3x10^3 A/mm^2 and τ = 1 μs (Fig. 4a). A decrease in the duration from 1 to 0.1 μs (Fig. 4b) and the density of a single current pulse below 3.0x10^3 A/mm^2 (Fig. 4c) causes a decrease in the stress jump amplitude down to its disappearance. In contrast, a transition from single pulse current to multiple pulses current sharply raises the stress jump amplitude up to 500 MPa (Fig. 4d).

A comparison of Figs. 3b and 4b demonstrates that an inflexion point (degeneration of plateau), corresponding to transformation, appears under the action of a current in the NC state before annealing.

Detailed studies of the nature of the temperature changes on the tensile samples with different structure refinement at single pulse current have revealed some features (Figs. 5 and 6). It can be observed that single pulses at different tension stages lead to stress jumps of various amplitudes and directions. However, the temperature increment from each pulse is no more than 45 °C, on the average 30 °C for the CC alloy and 15 °C for the NC alloy. This means that a weak temperature rise on the sample generates considerable stress changes. From Fig. 7 it can also be concluded that stress relaxation for jumps of both types is faster (15-20 s) than temperature relaxation (25-30 s). The jump upward relaxes more slowly (20 s) than the jump downward (15 s).

In Table 3 the mechanical properties of the CC and the NC alloy at tension with current are shown. Here, as well as at tension without current, grain refinement leads to a growth of strength and a decline in ductility. Post-deformation annealing promotes partial restoration of elongation to failure. It also appears that the pulse current influences the shape of stress-strain curves and ductility. A comparison of elongations to failure for the CC and the NC states in Tables 2 and 3 shows that their values at tension with current are 1.5-2 times higher than without current.

4. DISCUSSION

As a result of application of various deformation techniques, the microstructures, differing in grain size, type of intragranular defects, phase composition and crystallographic texture (Fig. 1) have been received

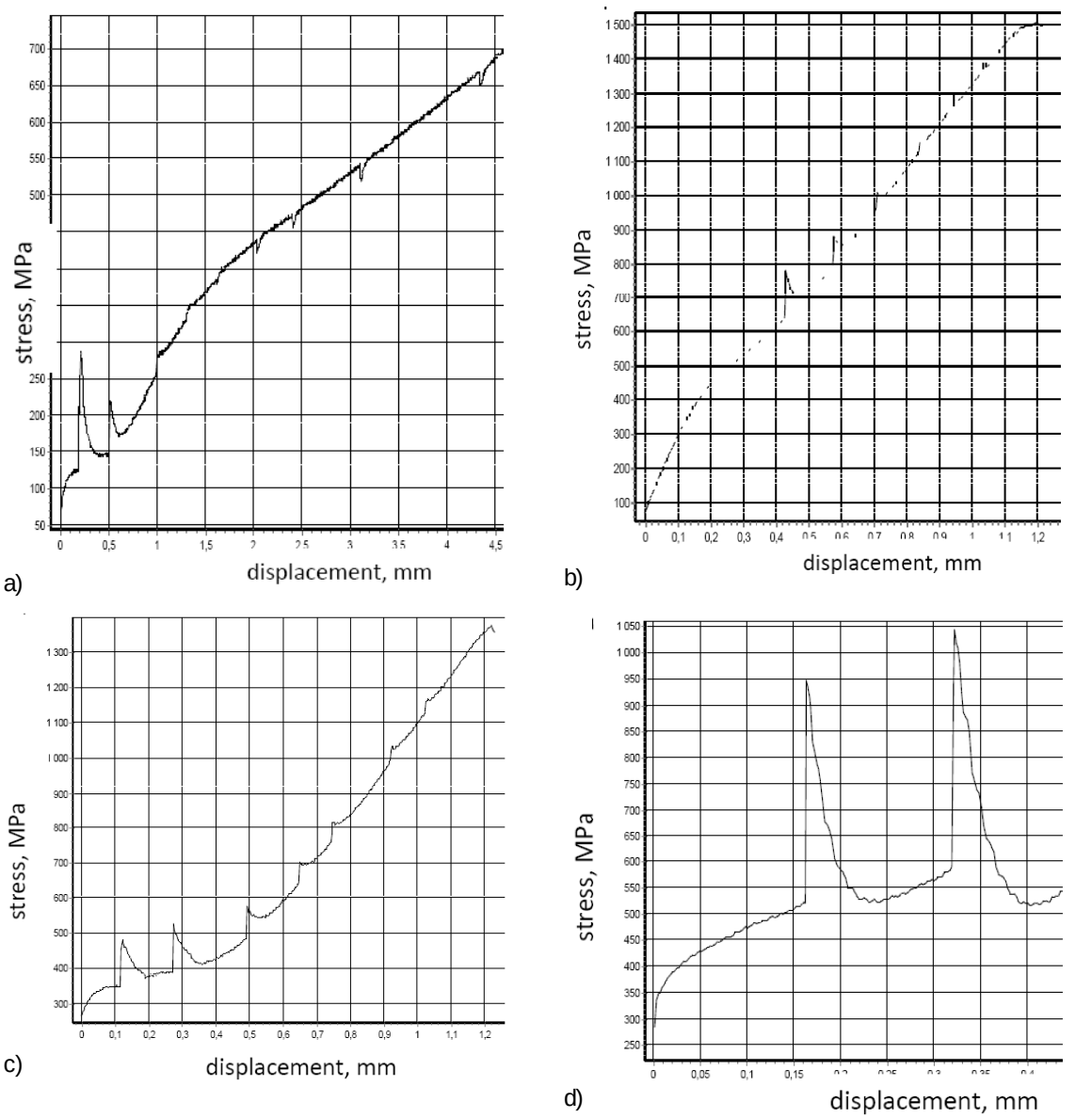

Fig. 4. Typical stress-strain curves at tension with single (a, b, c) pulse and multi-pulse (d) current for TiNi alloy in CG (a), EPR states before (b) and after annealing at 450 °C (c, d).

Table 3. Mechanical properties of $Ti_{49.3}Ni_{50.7}$ alloy at tension with current.

Treatment	State	grain size, [μm]	$\sigma_м$, [MPa]	YS, [MPa]	UTS, [MPa]	δ, [%]
Quenching from 800 °C	CC	50	150/210	400/600	750/940	60-80/40
EPR (*e*=1.81)	NC	0.08	450/-	1480/1587	1500/1926	5/2.4
EPR (*e*=1.81) + 450 °C		0.10	00/250	1170/1200	1300/1300	17/9.6

Numerator/denominator is the value for tension with/without current

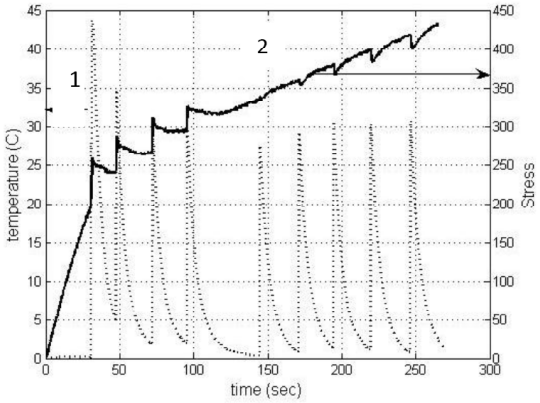

Fig. 5. Temperature changes (1) and stress jumps (2) in CC sample.

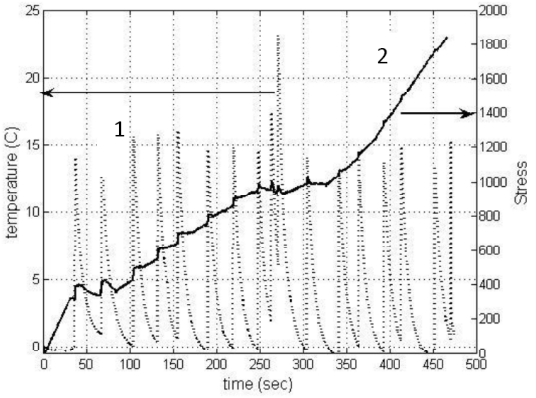

Fig. 6. Temperature changes (1) and stress jumps (2) in annealed NC sample.

in the TiNi alloy. Each of the mentioned structural features is capable of influencing the alloy ductility, raising or lowering it. For example, the absence of microtwins in the microstructure of the quenched CC alloy subjected to EPR has been revealed (Fig. 1b). It can be a potential for ductility growth. The important result is the fact that possible grain growth and degradation of the SMC structure has not been observed at electroplastic rolling of the ECAP-processed alloy. Moreover, electroplastic rolling promotes nanostructure formation with plenty of microtwins (Fig. 1c).

As it can be seen from Table 1, the strongest influence of a pulse current on alloy deformability has been revealed. Introduction of a pulse current in the deformation zone at cold rolling of the low-conducting intermetallic TiNi alloy raises deformability by two-three times in comparison with cold rolling without current (Table 1). The experimental data show that deformability with current grows not only for the CC but for the SMC state as well [11]. Besides, elevated deformability appears only after application of the critical current density j_{cr} = 84 and 160 A/mm^2, correspondingly. It is clear because the enhanced deformability has not been observed below these values. The critical value j_{cr} for CC TiNi is twice higher than the critical current density for commercially pure coarse-grained titanium in [12]. Taking into account the low electroconductivity of the intermetallic TiNi alloy, these results can be considered as comparable. The difference between the critical current density for the CC and the SMC alloys is conditioned by their different initial ductility (Table 2). The presence of the critical current den-

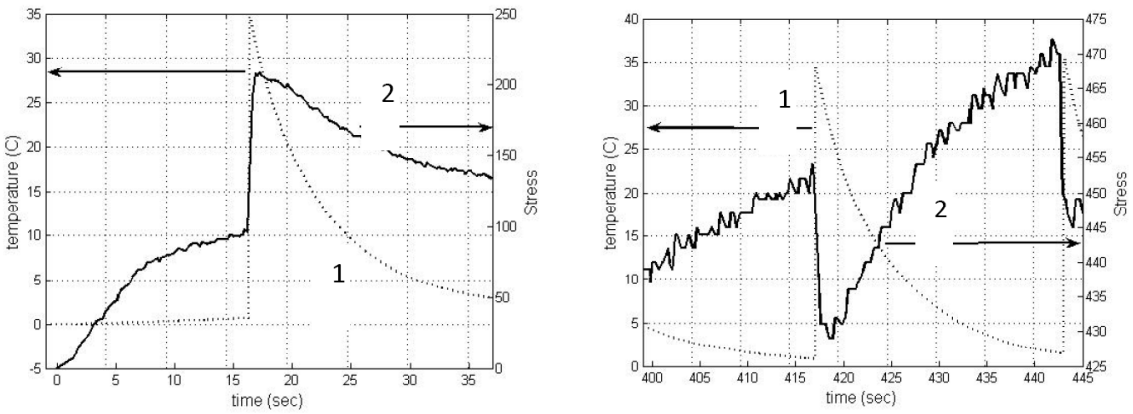

Fig. 7. Relaxation of temperature (curve 1) and stress (curve 2) at the beginning stage (a) and the final stage (b) at tension in CC (in expanded scale).

sity can be regarded as an argument for the nonthermal nature of the effect. This is also confirmed by direct temperature measurements by an infra-red chamber. It has been shown that the greatest possible temperature on the sample surface after multiple rolling does not exceed 150 °C. Taking into account the short duration (high velocity) of the process and immediate water cooling of the sample after each pass, it is possible to neglect the total thermal heating. Nevertheless, high local heating in the places of a microdefects cluster is possible. It is necessary to note that the electroplastic effect is for the first time observed on monocrystals or polycrystalline alloys without phase transformations [4,12].

For the TiNi alloy strong strain hardening is typical. That is why it assists brittle fracture in the absence of relaxation processes in structure and under large strain (Fig. 2a). Introduction of pulse current, apparently, leads to the interaction of electronic "wind" with pile-up of dislocation and structural relaxation that promotes the elevated deformability. The main reason of the appearance of microcracks during EPR is connected with the stress-strain state that changes from bulk triaxial to flat biaxial during thickness reduction of the sample (Fig. 2b). The experiments have also shown that removal of edge microcracks during EPR allows to increase the strain to failure.

The shape features of the stress-strain curves at tension of the TiNi alloy are caused by phase transformation (Fig. 3). The presence of the stress plateau at 210 and 294 MPa serves as the evidence of induced B2→B19 transformation (Figs. 3a, 3c). The plateau near 50 MPa for the NC state (Fig. 3c) can be connected with reorientation or reverse transformation of the B19 phase [13]. The absence of any plateau in Fig. 3b is connected with stabilization of martensite phases by EPR processing which can turn to austenite only under heating above 250 °C [14]. Common for all the curves is the absence of the necking stage. A high uniform elongation for the CC state (Fig. 3a) sharply contrasts with its absence in the NC state before and after annealing (Figs. 3b and 3c). Note that the total length of the plateau (ε_m) for the NC annealed state is maximum and twice higher than in the CC state. This testifies to a greater induced transformation ductility.

The data in Table 2 demonstrate that structure refinement of the TiNi alloy by deformation methods leads to a sharp reduction of ductility. A decrease of the grain size from tens of microns down to tens of nanometers reduces elongation to failure more than by one order. But a post-deformation annealing promotes partial restoration of ductility. The observable changes of ductility in the TiNi alloy with a reverse phase transformation do not differ from the mechanical behavior of metals and alloys without phase transformation [15,16]. This testifies to a generality of deformation mechanisms in alloys of different nature. Note that a decrease and an increase of ductility in the TiNi alloy is connected not only with a change of the grain size, but also with structure-phase transformations - partial amorphization due to severe plastic deformation and nanocrystallization at heating [8].

Due to the lack of publications on EPE in nanomaterials the possibility of the effect manifestation in nanostructured nitinol was not clear. Though the data given below related to EPE and its possible connection with enhancement of technological deformability in nitinol will be discussed for the first time, this question remains open and requires detailed investigations in the future.

The nature of the stress jumps on the stress-strain curves at tension with current is various and reflects a preferential manifestation of either phase transformations or the electroplastic effect. The stress jumps upward are connected with the reverse transformation M↔A which is stimulated with a current pulse and easy rise in temperature. The nature of such jumps is similar to the display of a reversible stress during the sample loading by tension. Since martensite in different quantities is present at all structural states during tension, stress jumps upward are also on all the tension curves. The jump amplitude dependence on the current density (Fig. 4a), pulse duration (Fig. 4b) and the number of pulses (Fig. 4d) is clear because an increase of the parameters leads to a rise in the sample temperature and accordingly, in the volume of the transformed phase. It should be noted that the absolute temperature values on the sample surface from single current pulses are very small in comparison with stress changes (Fig. 5). This may indicate the nonthermal nature of both jumps upward and jumps downward. The difference in temperature and stress relaxation kinetics, especially for jumps downward (Fig. 7), is also associated with different mechanisms responsible for jumping down and up.

Stress jumps downward in comparison with stress jumps upward have a noticeably smaller amplitude and, apparently, reflect the manifestation of EPE. In the stable state both martensite and austenite phases are capable structurally to relax under the action of a current. Thus EPE is observed only for the CC state. Probably, for release of dislo-

cation clusters and display of the EPE in the NC state higher current parameters are required.

The following important circumstance should be marked. Both kinds of stress jumps stimulate elevated ductility, which is connected with the induced phase transformation, and with usual dislocation mobility. It is visible in the increase in the length of the stress-plateau, occurrence of inflexion point and uniform elongation stage.

The pulse current has a positive influence on ductility not only in combination with cold rolling or tension but also when it operates independently during EPT as a source of Joule heating (Table 3). The efficiency of EPT processing consists in a multiple decrease in operational time and in achievement of the best combination of strength and ductility, in comparison with traditional annealing. It is possible to assume that direct heating by a pulse current selectively influences dislocation clusters and helps to form a homogeneous structure.

5. SUMMARY

The combination of electroplastic rolling and post-deformation annealing in a coarse-crystalline nickel-enriched TiNi alloys allows to generate a homogeneous nanostructure without deformation defects such as microtwins and dislocations.

Electroplastic rolling increases deformability of the $Ti_{49.3}Ni_{50.7}$ alloy by 1.5-3 times in the coarse-crystalline and the submicrocrystalline states.

Introduction of a pulse current during tension promotes enhancement of phase and dislocation ductility. Two different types of stress jumps during tension have been observed – jump upward and jump downward corresponding to the phase transformation and the electroplastic effect, accordingly.

Electropulse treatment instead of traditional annealing can improve ductility without a significant strength loss.

This work was supported by the Russian Foundation for Basic Research, grants # # 08-08-00497-a, 08-08-92202-China_a, and the Russian Federation Agency on Education, project 2.1.2./385. The author is grateful to Dr. Plekhov for his assistance in temperature measurements.

REFERENCES

[1] Y. Wang, M. Chen, F. Zhou and E. Ma // *Nature* **419** (2002) 912.
[2] C. Koch // *Scripta Mater*. **49** (2003) 657.
[3] R. Valiev// *Nature* **419** (2002) 887.
[4] O. Troitski, Yu. Baranov, Yu. Avraamov and A. Shlyapin, *Physical Fundamentals and Technologies of Treatment of Modern Materials* (Institute of Computer Researches, Moscow-Izhevsk, 2004).
[5] Y. Jiang, G. Tang, L. Guan, S. Wang, Z. Xu, C. Shek and Y. Zhu // *J. Mater. Res.* **23** (2008) 2685.
[6] V. Brailovski, S. Prokoshkin, P. Terriault, F. Trochu (Eds) *Shape Memory Alloys: Fundamentals, Modeling and Applications* (Quebec, Montreal, 2003).
[7] I. Khmelevskaya, S. Prokoshkin, I. Trubitsyna, M. Belousov, S. Dobatkin, E. Tatyanin, A. Korotitskiy, V. Brailovski, V. Stolyarov and E. Prokofiev // *Mater. Sci. Eng. A* **481-482** (2008) 119.
[8] V. Stolyarov, U. Ugurchiev, I. Trubitsyna, S. Prokoshkin and E. Prokofiev // *J. of High Pressure Physics and Technique* **4** (2006) 64.
[9] V. Pushin, V. Stolyarov, R. Valiev, T. Lowe and Y. Zhu // *Mater. Sci. Eng. A* **410–411** (2005) 386.
[10] V. Stolyarov, E. Prokofiev, S. Prokoshkin, S. Dobatkin, I. Trubitsyna, I. Khmelevskaya, V. Pushin and R. Valiev // *Phys. Met. Metallogr.* **100** (2005) 91.
[11] V. Stolyarov // *Trans Tech Publications, Switzerland Materials Science Forum* **584-586** (2008) 507.
[12] H. Conrad // *Mater. Sci. Eng*. *A* **287** (2000) 276.
[13] V. Stolyarov // *Mater. Sci. Eng. A* **503** 15 (2009) 18.
[14] I. Trubitsyna, S. Prokoshkin, A. Korotitsky, K. Inaekyan, V. Stolyarov, S. Makushev, I. Khmelevskaya, A. Chirkova, A. Bugaev, D. Levin and U. Ugurchiev // *J. of Functional Mater.* **1** (2007) 66.
[15] H. Gleiter // *Acta Mater.* **48** (2000) 1.
[16] R. Valiev, R. Islamgaliev and I. Alexandrov // *Progr. Mater. Sci*. **45 (2)** (2000) 103.